Biophysical Chemistry 141 (2009) 29–33

Contents lists available at ScienceDirect

Biophysical Chemistry

journal homepage: http://www.elsevier.com/locate/biophyschem

Hydrogen bonding versus stacking stabilization by modified nucleobases incorporated in PNA·DNA duplexes

Anjana Sen, Peter E. Nielsen *

Department of Cellular and Molecular Medicine, Faculty of Health Sciences, The Panum Institute, University of Copenhagen, Blegdamsvej 3c, DK-2200, Copenhagen N, Denmark

ARTICLE INFO

Article history:
Received 9 September 2008
Received in revised form 17 December 2008
Accepted 17 December 2008
Available online 31 December 2008

Keywords:
Modified base
Thermal melting
Thermodynamics
Sequence mismatch discrimination
PNA·DNA hybridization
Dimethyl formamide

ABSTRACT

The effects of incorporation of the modified nucleobases, 2,6-diaminopurine (D) (substituting for adenine) and 7-chloro-1,8-naphthyridin-2-(1*H*)-one (bicyclic thymine, bT) (substituting for thymine), that stabilize PNA·DNA duplex formation by increasing hydrogen bonding and/or base pair stacking interactions have been studied by thermal denaturation in terms of thermodynamics. Although the stabilizing effect of the bT base (in contrast to that of D base) is abolished upon addition of dimethyl formamide, thereby indicating that the stabilization is predominantly due to hydrophobic stacking forces, duplex stabilization was found to be enthalpic for both nucleobases. Increased stabilization (although not fully linearly) was observed with increasing numbers of modified bases, and single base sequence discrimination was only slightly compromised, but showed significant dependence on the sequence context.

1. Introduction

The stability of nucleobase double helices, such as those composed of DNA or RNA, is dependent on a combination of intrabasepair hydrogen bonding and interbasepair stacking interactions of which the latter provide the larger contribution to the free energy of duplex formation (in aqueous media) [1–5]. Thus, for a given duplex of a defined sequence, the stability may be increased by substituting the natural A, C, G and T nucleobases with modified nucleobases that are capable of base pairing with additional hydrogen bonds and/or with increased interbasepair stacking overlap. In attempts of creating oligonucleotide probes with increased affinity for their natural DNA or RNA targets within genetic diagnostics or genetic therapy (*e.g.* antisense technology), a variety of such modified nucleobases have been discovered and studied [6–15]. For instance, in the context of peptide nucleic acids (PNA), we have shown earlier that the adenine analogue, 2,6-diaminopurine (D), which can recognize thymine through three hydrogen bonds (as compared to only two in case of adenine) stabilizes PNA·DNA duplexes by 2–6 °C per substituted adenine [16]. In another study, we presented a bicyclic thymine analogue, 7-chloro-1,8-naphthyridin-2-(1*H*)-one (bicyclic T, bT) with increased surface area, which stabilizes PNA·DNA duplexes by more than 2 °C per substituted thymine [17].

In order to gain more insight into the mechanism of hydrogen bonding versus stacking stabilization of nucleobase helices, we have studied the hybridization of DNA with eight PNA oligomers containing single or multiple substitutions of D or bT in terms of T_m and hence derived thermodynamic parameters.

2. Materials and methods

2.1. PNAs

PNAs were synthesized using solid phase Boc chemistry, purified by HPLC and characterized by MALDI-TOF mass spectrometry as described previously [18]. Synthesis of PNA monomers containing D and bT bases and their incorporation in PNA oligomers have been described previously [16,17]. PNA concentrations were determined spectrophotometrically at 65 °C using molar extinction coefficients: ε_{260} of adenine = 15,400 M^{-1} cm^{-1}, ε_{260} of guanine = 11,700 M^{-1} cm^{-1}, ε_{260} of thymine = 8800 M^{-1} cm^{-1}, ε_{260} of cytosine = 7400 M^{-1} cm^{-1}, ε_{260} of D = 7600 M^{-1} cm^{-1} and ε_{260} of bT = 5500 M^{-1} cm^{-1}.

2.2. Chemicals and DNAs

All chemical reagents used were of analytical grade except for dimethyl formamide (DMF), which was spectroscopic grade from Sigma-Aldrich, Munich, Germany. The DNA oligonucleotides were purchased from DNA Technology (Aarhus, Denmark) and used without further purification.

2.3. Sample preparation

Main stock solutions of PNAs and DNAs were prepared by dissolution in deionized double distilled water. Experimental samples were made

* Corresponding author. Tel.: +45 35327762; fax: +45 32 39 6042.
E-mail address: ptrn@sund.ku.dk (P.E. Nielsen).

0301-4622/$ – see front matter © 2008 Elsevier B.V. All rights reserved.
doi:10.1016/j.bpc.2008.12.006

Table 1
PNA and DNA sequences

Strands	Sequence[a,b]	Base composition[c,d]
PNA1	H-(eg1)$_2$-AGA GTC AGC TT-Lys-NH_2	$A_3G_3T_3C_2$
PNA2[c]	H-(eg1)$_2$-**D**GA GTC AGC TT-Lys-NH_2	$DA_2G_3T_3C_2$
PNA3	H-(eg1)$_2$-**DGD** GTC AGC TT-Lys-NH_2	$D_2A_1G_3T_3C_2$
PNA4	H-(eg1)$_2$-**DGD** GTC **D**GC TT-Lys-NH_2	$D_3G_3T_3C_2$
PNA5[d]	H-(eg1)$_2$-AGA G(**bT**)C AGC TT-Lys-NH_2	$A_3G_3T_2(bT)C_2$
PNA6	H-(eg1)$_2$-AGA G(**bT**)C AGC (**bT**)T-Lys-NH_2	$A_3G_3T(bT)_2C_2$
PNA7	H-(eg1)$_2$-AGA G(**bT**)C AGC (**bT**)(**bT**)-Lys-NH_2	$A_3G_3(bT)_3C_2$
PNA8	H-(eg1)$_2$-AG**D** G(**bT**)C **D**GC (**bT**)T-Lys-NH_2	$D_2AG_3T(bT)_2C_2$
PNA9	H-(eg1)$_2$-AAG CTG ACT CT-Lys-NH_2	$A_3G_2T_3C_3$
DNA1	5′-AAG CTG ACT CT-3′	$A_3G_2T_3C_3$
DNA2	5′-AAG CTG **G**CT CT-3′	$A_2G_3T_3C_3$
DNA3	5′-AAG CTG $\overline{C}$CT CT-3′	$A_2G_2T_3C_4$
DNA4	5′-AAG CTG $\overline{A}$C**G** CT-3′	$A_3G_3T_2C_3$
DNA5	5′-AAG CTG AC$\underline{\overline{C}}$ CT-3′	$A_3G_2T_2C_4$

[a] All the duplexes resulting from these sequences would be anti-parallel (either N/C or N/3′ or 5′/3′).
[b] The N-terminal of the peptide backbone of PNA is shown by an H and the C-terminal (amidated carboxyl terminal) of the peptide backbone of PNA is shown by an NH_2.
[c] D ≡ 2,6-diaminopurine.
[d] bT ≡ 7-chloro-1,8-naphthyridin-2-(1*H*)-one.

by diluting from the corresponding main stock solutions in 10 mM phosphate buffer (pH 7.2) containing 100 mM NaCl and 0.1 mM EDTA.

Equimolar mixtures (1:1 stoichiometry in single strands) of the PNA or DNA and its complementary strand were dissolved in the buffer mentioned above. The duplex formation was assured by heating to 90 °C and then cooling slowly to room temperature to allow proper annealing. No sign of aggregation or decreased solubility of the PNAs at up to 70% of organic co-solvents was observed.

2.4. UV-melting experiments

The thermal melting experiments were performed on a Cary 300 Bio UV–visible spectrophotometer (Varian, Cary, NC, USA) attached to a temperature controller. Thermal melting profiles were obtained using heating-cooling cycles in the range of −3 °C to 95 °C. The melting temperature (T_m) was determined from the peak of the first derivative of the heating curve. Cuvettes of 1.0 cm path length and 1.0 ml volume were used for all experiments.

It is important to note that thermal denaturation curves showed essentially unperturbed monophasic behaviour up to 60% organic co-solvent. (Thermal melting curves in the presence of >60% of DMF start to lose the upper baseline and show severe disturbances, partly because of high absorbance of DMF at the wavelength required for the experiments. Therefore, thermal or thermodynamic data at >60% of DMF could not be obtained.)

2.5. Thermodynamics

The thermodynamic parameters viz enthalpy change (ΔH^0), entropy change (ΔS^0), and Gibbs' free energy change (ΔG^0) were evaluated using the hyperchromicity method (curve fitting) and/or the concentration method [19,20].

2.6. The hyperchromicity method

The hyperchromicity method utilizes alpha curve and van't Hoff plots ($\ln K_T$ versus T^{-1}) according to the following definitions: The fraction (α_T) of the single strands that remained hybridized in the duplex at a particular temperature T in Kelvin is represented as:

$$\alpha_T = \frac{A_s - A}{A_s - A_d} \tag{1}$$

where, A_d is the absorbance of the duplex in fully hybridized condition, A_s is the absorbance of the single strands in fully denatured condition and A is absorbance at a particular point on the thermal melting curve at temperature T.

For non-self complementary sequences forming n-mer structures, the general equilibrium constant (K_T) at a particular temperature T can be expressed as [19,20]:

$$K_T = \frac{\alpha_T}{(1-\alpha_T)^n \left(\frac{c_{ts}}{n}\right)^{n-1}} \tag{2}$$

where, c_{ts} represents the total concentration of strands and n is the molecularity of the complex. Assuming a two-state model, Eq. (2) reduces to

$$K_T = \frac{2\alpha_T}{(1-\alpha_T)^2 c_{ts}}. \tag{3}$$

The van't Hoff plot $\ln K_T$ versus T^{-1} is a straight line represented by

$$\ln K_T = \left(-\frac{\Delta H^0}{R}\right)\frac{1}{T} + \left(\frac{\Delta S^0}{R}\right). \tag{4}$$

Hence, ΔH^0 can be obtained from the slope and ΔS^0 can be obtained from the Y-intercept of the van't Hoff plot. ΔG^0 at a particular temperature T (K) can be calculated from

$$\Delta G^0 = -RT \ln K_T = \Delta H^0 - T\Delta S^0 \tag{5}$$

where R, the universal gas constant is 1.986 cal/mol K.

2.7. The concentration method

The concentration method utilizes a plot of T_m^{-1} versus $\ln c_{ts}$, where T_m is the thermal melting temperature of the duplex and c_{ts} is the total strand concentration of PNA or DNA [19,20].

Since T_m is defined by the temperature where α=0.5 for a two state transition, combining Eqs. (3) and (4) yields:

$$\frac{1}{T_m} = \frac{R}{\Delta H^0}\ln c_{ts} + \frac{\Delta S^0 - R\ln 4}{\Delta H^0} \tag{6}$$

Thus the thermodynamic parameters can be extracted from a linear fit to a plot of T_m^{-1} versus $\ln c_{ts}$ according to Eq. (6). Hence, ΔH^0 is obtained from the slope of the linear fit and ΔS^0 from the Y-intercept.

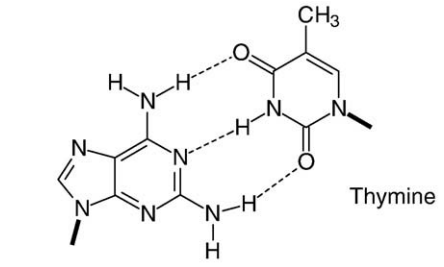

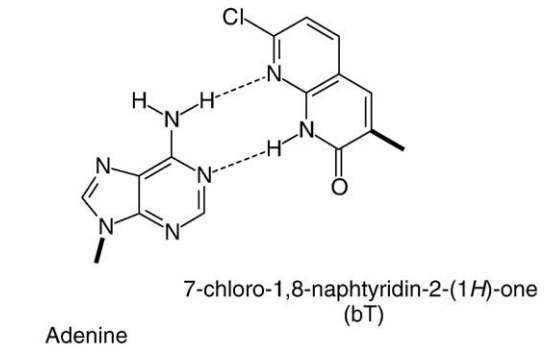

Fig. 1. Base paring of thymine with 2,6-diamonipurine (D), and adenine with 7-chloro-1,8-naphthyridin-2-(1*H*)-one (bT).

Table 2
Summary of thermal results of fully matched PNA·DNA duplexes

Strands	T_m (°C)[a,b]	T_m^{-1} versus lnc_{ts} plot[c]			van't Hoff plot[b,d]			ΔC_p[e] (kcal/mol K)
		ΔG^0_{37} (kcal/mol)	ΔH^0 (kcal/mol)	ΔS^0 (cal/mol K)	ΔG^0_{37} (kcal/mol)	ΔH^0 (kcal/mol)	ΔS^0 (cal/mol K)	
PNA1·DNA1	67.1±0.2	−15.4	−82.3	−216.0	−14.7±0.5	−80.3±0.8	−212.4±7.2	0.50
PNA2·DNA1	68.3±0.5	−15.8	−85.3	−223.8	−15.2±0.3	−83.0±1.1	−218.7±6.5	0.12
PNA3·DNA1	73.4±0.4	−16.6	−87.5	−227.6	−16.4±0.3	−86.8±0.5	−227.0±5.3	0.37
PNA4·DNA1	77.1±0.4	−18.4	−90.8	−233.3	−18.4±0.4	−89.7±1.2	−230.2±4.7	0.80
PNA5·DNA1	69.2±0.3	−16.0	−86.7	−226.3	−15.4±0.2	−84.5±0.9	−222.7±7.7	0.50
PNA6·DNA1	70.2±0.5	−16.5	−87.5	−229.1	−16.2±0.5	−87.2±0.8	−229.3±6.3	0.96
PNA7·DNA1	71.2±0.3	−17.8	−91.4	−238.2	−16.7±0.4	−91.7±0.8	−240.0±4.2	0.90
PNA8·DNA1	79.2±0.3	−19.4	−95.2	−244.2	−19.0±0.3	−95.8±0.7	−247.6±4.5	0.45

[a] The melting temperatures presented correspond to a duplex concentration of 5.0 μM in strands (c_{ts} = 10.0 μM). The solvent was 10 mM phosphate buffer containing 100 mM NaCl and 0.1 mM EDTA, pH 7.2±0.01.
[b] Three independent measurements were used to calculate the standard deviation.
[c] Evaluated from a plot of T_m^{-1} versus lnc_{ts} fitted to Eq. (6) evaluated in a range of 1.0–10.0 μM of strand concentration (Figs. S2–S3).
[d] Evaluated from hyperchromicity (curve fitting) method [see the Results and discussion section].
[e] Extraction of thermodynamic parameters derived from thermal melting method requires that no/minimum change in heat capacity occurs in the duplex-single strand equilibrium. For the present systems we have found only minor changes.

The values of the thermodynamic parameters calculated by this method are thus independent of strand concentration, which is not the case with the hyperchromicity method described above.

3. Results and discussion

The sequences of the PNA and DNA oligomers used in this study are listed in Table 1, and the molecular structures of the modified bases are depicted in Fig. 1. In order to perform a complete thermodynamic analysis, thermal denaturation curves of the PNA·DNA duplexes were obtained, and from these data the thermodynamics parameters viz. enthalpy change (ΔH^0), entropy change (ΔS^0) and Gibbs' free energy change (ΔG^0) were derived using both the hyperchromicity method (curve fitting) as well as the concentration method (T_m^{-1} versus lnc_{ts} plot, Eq. (6)). (Representative thermal melting curves are displayed in Fig. S1. A distinctive decrease in hyperchromicity observed in these curves with the increase in the number of modified bases is ascribed to differences in stacking hyperchromicity of the natural nucleobases compared to that of the modified bases D and bT.) The thermal and thermodynamic data are shown in Table 2 (the corresponding T_m^{-1} versus lnc_{ts} plots are shown in Figs. S2 and S3).

The presence of one, two or three D bases at specific positions in the PNA strand increased the melting temperature of the PNA·DNA duplex by 1.2, 6.3 and 10.0 °C, respectively, compared to that of the control (unmodified) duplex (Table 2). Analogously, the presence of one, two or three bT bases in the PNA strand increased the melting temperature of the PNA·DNA duplex by 2.1, 3.1 and 4.1 °C, respectively (Table 2).

The presence of a combination of both D and bT bases in the PNA strand (PNA8, two bT and two D) increased the thermal stability of the PNA·DNA duplex by 9 °C, compared to the PNA with only two bT (PNA6).

The effect on thermal stability of increasing number of D bases in the PNA is not linear, (most likely because of sequence context effects (nearest neighbour effects)), whereas the incremental T_m effect of multiple bT substitutions appears fairly uniform, even when placed in adjacent positions (PNA6 compared with PNA7).

The obtained values of free energy change (ΔG^0) of duplex formation show reasonably good correspondence to the thermal melting temperatures, and duplex formation is enthalpically driven in all cases. Furthermore, upon incorporation of the D and bT nucleobases, the additional free energy obtained is also due to an increased enthalpic contribution. Although the individual differences within the series of nucelobase substituted PNAs are quite small, the overall trend upon increasing substitution is very clear, and very similar results are also found through curve fitting as well as concentration dependence determinations, thereby significantly strengthening the above conclusion. This observation is compatible with the notion that the stabilization by D base is through an extra hydrogen bond, but somewhat surprising in case of the bT nucleobase for which stabilization is through increased stacking (water exclusion) (which is also demonstrated by the effects on duplex stability by the presence of organic solvent DMF) (see below).

3.1. Effect of DMF

The behaviour of PNA duplexes containing modified bases in a non-aqueous environment gives a more direct molecular perspective of the relative contributions of the stabilizing forces. In a previous study on the effect of the aprotic, organic solvent DMF on the stability of iso-sequential PNA·PNA, PNA·DNA and DNA·DNA duplexes, we have shown that the change in the number of bound water molecules associated upon thermal melting of PNA·PNA duplexes is the smallest [21], and that PNA duplexes (in contrast to DNA duplexes) show almost unaffected stability in 70% DMF [22]. In order to assess the contributions from stacking forces and H-bonds to the thermal stability of the duplexes of the present study, we have investigated the effect of increasing amount of DMF on the thermal stabilities of the PNA duplexes containing D base and/or bT base (Fig. 2; thermal and thermodynamic data are presented in Tables S2–S6 with representative thermal melting curves in Figs. S4 and S5, and the corresponding plots in Fig. S6). It is striking, that whereas the destabilizing effect of increasing amount of DMF on the PNA duplex containing three D bases

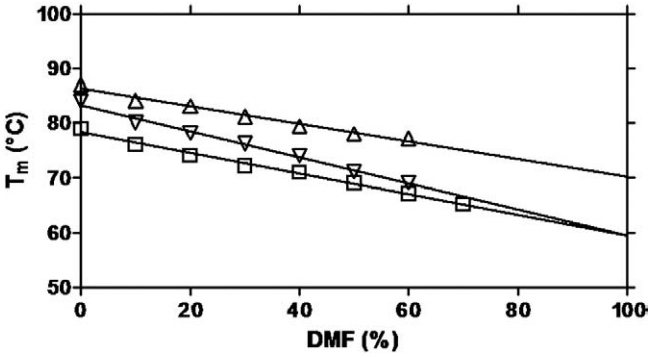

Fig. 2. Effect of DMF on the stabilities of the PNA duplexes containing modified bases in comparison to the control (unmodified) duplex. T_m of PNA duplexes PNA1·PNA9 (—□—), PNA4·PNA9 (—△—) and PNA7·PNA9 (—▽—) as a function of increasing amount of DMF in the medium. Data are from Tables S2–4 (summarized in Table S6). The duplex concentration is 5.0 μM in strands. The amount of DMF was vol.% in 10 mM phosphate buffer containing 100 mM NaCl and 0.1 mM EDTA, pH 7.2±0.01.

Table 3
Thermal melting temperatures of the PNA·DNA duplexes containing single base mismatches in the DNA strand

PNA strands	Mismatch dG7[a]		Mismatch dC7[b]		Mismatch dG9[c]		Mismatch dC9[d]	
	T_m (°C)[e,f]	$-\Delta T_m$ (°C)[g]	T_m (°C)[e,f]	$-\Delta T_m$ (°C)[g]	T_m (°C)[e,f]	$-\Delta T_m$ (°C)[g]	T_m (°C)[e,f]	$-\Delta T_m$ (°C)[g]
PNA1	54.3±0.4	12.8	51.1±0.3	16.0	51.1±0.2	16.0	52.1±0.2	15.0
PNA2	58.1±0.3	10.2	55.1±0.2	13.2	54.2±0.2	14.1	55.1±0.4	13.2
PNA3	62.1±0.5	11.3	59.2±0.2	14.2	54.0±0.5	19.4[h]	61.2±0.2	12.2
PNA4	67.2±0.2	9.9	65.3±0.4	11.8	60.3±0.4	16.8[h]	68.3±0.3	8.8
PNA5	56.0±0.2	13.2[h]	56.4±0.5	12.8	53.4±0.5	15.8	55.3±0.3	13.9
PNA6	58.1±0.4	12.1	58.0±0.4	12.2	55.0±0.3	15.2	58.0±0.5	12.2
PNA7	61.2±0.3	10.0	59.1±0.2	12.1	62.1±0.4	9.1	59.1±0.4	12.1
PNA8	68.4±0.3	10.8	68.1±0.3	11.1	66.1±0.2	13.1	67.1±0.5	12.1

[a] PNAs hybridized with DNA2 (with mismatch dG7).
[b] PNAs hybridized with DNA3 (with mismatch dC7).
[c] PNAs hybridized with DNA4 (with mismatch dG9).
[d] PNAs hybridized with DNA5 (with mismatch dC9).
[e] The melting temperatures presented correspond to a duplex concentration of 5.0 μM in strands (c_{ts} = 10.0 μM). The solvent was 10 mM phosphate buffer containing 100 mM NaCl and 0.1 mM EDTA, pH 7.2±0.01.
[f] Three independent experiments were used to calculate the standard deviation.
[g] The '−' sign indicates a decrease in the value with respect to that of the corresponding fully matched PNA·DNA duplex.
[h] See the Results and discussion section.

is fully parallel to that of the unmodified PNA duplex, the additional stability of the PNA duplex containing three bT bases showed a steady decrease with increasing amount of DMF up to 60% of DMF, and it is totally abolished when extrapolated to 100% DMF (Fig. 2). These results fully support the conclusion that the D·T base pair behaves like a normal base pair (in essence like a G·C base pair), being stabilized by hydrogen bonding as well as stacking forces, while the additional stabilization offered by the bicyclic thymine analogue bT appears to be exclusively of hydrophobic stacking nature.

3.2. Single base sequence discrimination by D base or bT modifications

In order to study whether sequence discrimination was compromised by the introduction of the D or bT bases, thermal stabilities were measured for PNA·DNA duplexes containing single mismatches (G or C bases) in the DNA strand at positions 3 or 5 of the PNA strand across from positions substituted with D or bT base, respectively.

The results (Table 3, summarized in Table S7 with corresponding T_m^{-1} versus $\ln c_{ts}$ plots shown in Fig. S7, and a bar diagram representation shown in Fig. S8) show that all mismatches as expected cause destabilization of the duplex, but with significant variations (Table 3). For example, the destabilization of the PNA·DNA duplex caused by a G7 mismatch is less in the presence of a combination of two D bases and two bT bases compared to the unmodified duplex. In general, the stability of the PNA·DNA duplexes containing modified bases appear slightly less sensitive to base pair mismatches, compared to the unmodified PNA·DNA duplexes. Although both thermodynamic and structural factors determine mismatched duplex stabilities, G·G and G·T mismatches are in general identified as the most stable mismatches, whereas C·C is the least stable one [20]. Clear experimental evidence for the influence of sequence context beyond nearest neighbour effects on the thermodynamic stability of a single base pair mismatched DNA duplex has been reported [23]. In the presently described PNA·DNA context, destabilization due to mismatches is clearly affected by the type of mismatch (G·T versus C·T and G·A versus C·A), the nucleobase partner (adenine versus diaminopurine and thymine versus bicyclic thymine), as well as the sequence context (nearest neighbour effects). However, the present (limited) data do not allow a full picture concerning the relative contributions of these factors.

Nonetheless a closer scrutiny of the data in Table 3 reveals that a T·C mismatch at position 7 destabilizes the unmodified PNA·DNA duplex more than a T·G mismatch at the same position (PNA1·DNA2 versus PNA1·DNA3), whereas destabilizations of the unmodified PNA·DNA duplex by A·G and A·C mismatches at position 9 are quite close (PNA1·DNA4 versus PNA1·DNA5).

With increasing number of D bases, the effect of T·G and T·C mismatches at position 7 (dG7 and dC7) is comparable. However, improved discrimination occurs when the D base is confronting a G mismatch (dG9) at position 9 (PNA3·DNA4), but this is not the case with a C mismatch at the same position (dC9), most likely reflecting the poor fit of two opposing purines combined with the loss of the three D·T base pair hydrogen bonds.

On the other hand, the data indicate that the bT base is relatively insensitive to the mismatch type and position in contrast to the D base, reflecting that the stabilization by this base is predominantly (or exclusively) due to increased base stacking.

The discrimination related to an A·G mismatch (a purine·purine pair, dG9) at position 9 in PNA5·DNA4 (one bT base) and PNA6·DNA4 (two bT bases) is almost as high as that seen for the unmodified duplex PNA1·DNA4. However, this discrimination is absent in the presence of two adjacent bT bases (PNA7·DNA4). This effect is ascribed to the increased stacking interactions, since it is not the case with the A·C mismatch (a purine·pyrimidine pair).

4. Conclusions

The present results clearly show that increased PNA·DNA hybridization stability (with only slight decrease in sequence discrimination) both in terms of thermal stability as well as in terms of Gibbs' free energy change is obtained by substitution of adenine and thymine bases with D and bT bases, respectively, in the PNA oligomer. The results furthermore show that the stabilizing effect of the bT base is predominantly (or exclusively) of hydrophobic (stacking) nature in contrast to that of the D base. Overall, the results emphasize the utility of these modified nucleobases in the design of PNA probes for diagnostic or gene therapeutic applications.

Acknowledgements

This work was supported by the European Commission, 6th Framework Programme, contract no IST 002035 PACE project, and the Danish Natural Science Foundation.

Appendix A. Supplementary data

Supplementary data associated with this article can be found, in the online version, at doi:10.1016/j.bpc.2008.12.006.

References

[1] E. Protozanove, P. Yakovchuk, M.D. Frank-Kamenetskii, Stacked-unstacked equilibrium at the nick site of DNA, J. Mol. Biol. 342 (2004) 775–785.
[2] P. Yakovchuk, E. Protozanove, M.D. Frank-Kamenetskii, Base-stacking and base-pairing contributions into thermal stability of the DNA double helix, Nucleic Acids Res. 34 (2006) 564–574.
[3] E.T. Kool, Hydrogen bonding, base-stacking and steric effects in DNA replication, Annu. Rev. Biophys. Biomol. Struct. 30 (2001) 1–22.
[4] C. Oostenbrink, W.F. van Gunsteren, Efficient calculation of many stacking and pairing free energies in DNA from a few molecular dynamics simulations, Chemistry 11 (2005) 4340–4348.
[5] M. Sundaralingam, P.K. Ponnuswamy, Stability of DNA duplexes with Watson–Crick base pairs: a predicted model, Biochemistry 43 (2004) 16467–16476.
[6] M.H. Moore, L. Van Meervelt, S.A. Salisbury, P.K. Lin, D.M. Brown, Direct observation of two base-pairing modes of a cytosine–thymine analogue with guanine in a DNA Z-form duplex: significance for base analogue mutagenesis, J. Mol. Biol. 251 (1995) 665–673.
[7] M.D. Kirnos, I.Y. Khudyakov, N.I. Alexandrushikina, B.F. Vanyushin, 2-Aminoadenine is an adenine substituting for a base in S-2L cyanophage DNA, Nature 270 (1977) 369–370.
[8] E.T. Kool, Preorganization of DNA: design principles for improving nucleic acid recognition by synthetic oligonucleotides, Chem. Rev. 97 (1997) 1473–1487.

[9] J.-A. Ortega, J.R. Blas, M. Orozco, A. Grandas, E. Pedroso, J. Robles, Binding affinities of oligonucleotides and PNAs containing phenoxazine and G-clamp cytosine analogues are usually sequence-dependent, Org. Lett. 9 (2007) 4503–4506.
[10] W.M. Flanagan, R.W. Wagner, D. Grant, K.-Y. Lin, M.D. Matteucci, Cellular penetration and antisense activity by a phenoxazine-substituted heptanucleotide, Nat. Biotechnol. 17 (1999) 48–52.
[11] W.M. Flanagan, J.J. Wolf, P. Olson, D. Grant, K.-Y. Lin, R.W. Wagner, M.D. Matteucci, A cytosine analog that confers enhanced potency to antisense oligonucleotides, Proc. Natl. Acad. Sci. U. S. A. 96 (1999) 3513–3518.
[12] C. Ausín, J.-A. Ortega, J. Robles, A. Grandas, E. Pedroso, Synthesis of amino- and guanidine-G-clamp PNA monomers, Org. Lett. 4 (2002) 4073–4075.
[13] K.G. Rajeev, M.A. Maier, E.A. Lesnik, M. Manoharan, High-affinity peptide nucleic acid oligomers containing tricyclic cytosine analogues, Org. Lett. 4 (2002) 4395–4398.
[14] P. Sazani, A. Astriab-Fischer, R. Kole, Effects of base modifications on antisense properties of 2′-*O*-methoxyethyl and PNA oligonucleotides, Antisense Nucleic Acid Drug Dev. 13 (2003) 119–128.
[15] K.C. Engman, P. Sandin, S. Osborne, T. Brown, M. Billeter, P. Lincoln, B. Nordén, B. Albinsson, L.M. Wilhelmsson, DNA adopts normal B-form upon incorporation of highly fluorescent DNA base analogue tC: NMR structure and UV–vis spectroscopy characterization, Nucleic Acids Res. 32 (2004) 5087–5095.
[16] G. Haaima, H.F. Hansen, L. Christensen, O. Dahl, P.E. Nielsen, Increased DNA binding and sequence discrimination of PNA oligomers containing 2,6-diaminopurine, Nucleic Acids Res. 25 (1997) 4639–4643.
[17] A.B. Eldrup, C. Christensen, G. Haaima, P.E. Nielsen, Substituted 1,8-naphthyridin-2 (1H)-ones are superior to thymine in the recognition of adenine in duplex as well as triplex structures, J. Am. Chem. Soc. 124 (2002) 3254–3262.
[18] L. Christensen, R. Fitzpatrick, B. Gildea, K. Petersen, H.F. Hansen, T. Koch, M. Egholm, O. Buchardt, P.E. Nielsen, J. Coull, R. Berg, Solid-phase synthesis of peptide nucleic acids, J. Pept. Sci. 1 (1995) 175–183.
[19] L.A. Marky, K.J. Breslauer, Calculating thermodynamic data for transitions of any molecularity from equilibrium melting curves, Biopolymers 26 (1987) 1601–1620.
[20] N. Peyret, P.A. Seneviratne, H.T. Allawi, J. SantaLucia Jr., Nearest-neighbor thermodynamics and NMR of DNA sequences with internal A A, C C, G G and T T mismatches, Biochemistry 38 (1999) 3468–3477.
[21] A. Sen, P.E. Nielsen, On the stability of peptide nucleic acid duplexes in the presence of organic solvents, Nucleic Acids Res. 35 (2007) 3367–3374.
[22] A. Sen, P.E. Nielsen, Unique properties of purine·pyrimidine asymmetric PNA·DNA duplexes by purines in the PNA strand, Biophys. J. 90 (2006) 1329–1337.
[23] T.S. Hall, P. Pancoska, P.V. Riccelli, K. Mandell, A.S. Benight, Sequence context and thermodynamic stability of a single base pair mismatch in short deoxyoligonucleotide duplexes, J. Am. Chem. Soc. 123 (2001) 11811–11812.